Paramagnetic Meissner effect in high-temperature superconductors

W. Braunisch, N. Knauf, G. Bauer, A. Kock, A. Becker, B. Freitag,
A. Grütz, V. Kataev,* S. Neuhausen, B. Roden, D. Khomskii,† and D. Wohlleben‡
II. Physikalisches Institut, Universität zu Köln, Zülpicher Strasse 77, D-50937 Köln, Germany

J. Bock and E. Preisler
Hoechst AG, Werk Knapsack, D-50354 Hürth, Germany
(Received 29 December 1992; revised manuscript received 2 April 1993)

We have studied the low-field Meissner effect of polycrystalline Bi high-temperature superconductors using a special superconducting-quantum-interference-device magnetometer. In certain samples a surprising feature was observed: Instead of the usual diamagnetic moment a paramagnetic moment develops in the field cooling mode below T_c for fields $H < 1$ Oe. The data are consistent with orbital paramagnetic moments due to spontaneous currents. Such currents may originate in so-called π contacts in the weak-link network of polycrystalline material. In some of these samples also an anomaly in the low-field microwave absorption was observed, which is obviously correlated with the existence of spontaneous currents.

I. INTRODUCTION

The Meissner effect of ceramic granular high-temperature superconductors (HTS's) is known to be incomplete even for fields $H < H_{c1}$ (usually of the order of $\frac{1}{3}$ of complete flux expulsion). This incompleteness is explained by flux pinning (e.g., see Ref. 1) and/or by the anisotropy of the London penetration depth (leading to the value $\frac{1}{3}$ for the flux expulsion; see Refs. 2–4). For very low fields of order 1 Oe or lower, the field-cooled (FC) susceptibility often tends toward full flux expulsion with decreasing field,[5,6] but also a reduction of the FC susceptibility in very low fields has been reported.[7] This field dependence is attributed to flux pinning and/or to the weak-link structure of the granular samples.[1–6]

In order to study this low-field behavior of the field-cooled susceptibility, we use a special superconducting-quantum-interference-device (SQUID) magnetometer as described in Sec. III. The most striking result of this research is the observation of a *paramagnetic* susceptibility below T_c: In certain particular melt-processed samples of the Bi-based HTS's, the FC susceptibility not only decreases with decreasing field, but even becomes *paramagnetic* below T_c in very low fields. In this paper we will call this behavior the "paramagnetic Meissner effect" (PME), although the use of the expression "Meissner effect," which is commonly associated with flux *expulsion,* may probably be somewhat confusing in this context. However, since we attribute the PME to the occurrence of spontaneous currents just like the ordinary Meissner effect, which also develops as a result of spontaneous currents (which flow, of course, in the opposite direction), we claim that this expression is justified in a certain sense.

We note that observations of paramagnetic moments in HTS's in the field-cooled mode have occasionally been seen and published in the literature.[8–10] The results of the FC susceptibility reported in Ref. 8 are very similar to our observations, which will be presented in detail in Sec. IV. In Ref. 8 the effect was attributed to a pinning effect in a Kosterlitz-Thouless transition. A metastable PME (the magnetization depends on the cooling speed) was observed in Y-doped Bi 2:2:1:2 (Ref. 11) (we note that such a dependence on the cooling speed was not observed in our undoped Bi 2:2:1:2 samples). Furthermore, we have recently learned that at the Universität Hamburg observations on Bi 2:2:1:2 (also melt-processed samples) were made, which are similar to ours.[12] At the Freie Universität Berlin, the PME was observed using a vibrating-sample magnetometer[13] on the same kind of samples, and at the Universität Karlsruhe a PME was found in some Y 1:2:3 single crystals.[14]

The main results of our own investigations have recently been published briefly in Ref. 15. In the present paper, we will give a detailed description of these results and will include more recent measurements.

II. SAMPLE PREPARATION AND CHARACTERIZATION

All samples presented in this paper are of the Bi-Sr-Ca-Cu-O system, prepared by different processing techniques. They were partly prepared at our laboratory,[16,17] by Hoechst AG (Hürth),[18,19] and at the Institut für Anorganische Chemie (Universität zu Köln).[20,21]

Samples Ne41T10B ($Bi_{1.8}Pb_{0.2}Sr_2CaCu_2O_y$ and Kn75KA ($Bi_{1.73}Pb_{0.27}Sr_2Ca_2Cu_3O_y$) were prepared by a standard sintering process; i.e., appropriate ingots of analytical grade (≥ 99–99.9%) Bi_2O_3, PbO, $SrCO_3$, $CaCO_3$, and CuO corresponding to the desired composition were thoroughly mixed in an agate mortar. These mixtures were prereacted in aluminum oxide crucibles in air at 780–790 °C for at least 48 h with intermediate grindings. The materials were then reground and pressed into pellets. These pellets were annealed in a slow gas stream as follows.

Sample Ne41T10B was annealed at 850 °C for 60 h in an Ar(92%)/O_2(8%) atmosphere to support the formation of the Bi 2:2:1:2 phase and at 690 °C for 10 h in an Ar atmosphere to shift its T_c above 90 K (see Ref. 16). Sample Kn75KA was annealed near the melting point of this stoichiometry at 860 °C for 370 h in an Ar(92%)/O_2(8%) atmosphere with intermediate grinding to support the formation of the Bi 2:2:2:3 phase. Note that it was partially melted during this main reaction. Afterwards, the sample was powdered and additionally annealed at 690 °C for 40 h in an O_2 atmosphere.

Sample KnBock1 ($Bi_2Sr_2CaCu_2O_x$) was manufactured by a melt-cast process (MCP); i.e., appropriate amounts of Bi_2O_3, SrO, CaO, and CuO were mixed, transferred to aluminum oxide crucibles, and then heated to 1030 °C (for $\frac{1}{2}$ h), until the mixture was completely molten, and then poured into a copper mold. The ingot was then removed from the mold and annealed at 770 °C for 24 h and at 850 °C for 120 h in air.[18,19] Five pieces of this sample (named KnBock2–KnBock6) were additionally annealed at 690–750 °C for 20–150 h in an Ar and/or O_2 atmosphere in order to vary the oxygen content.[17,22,23] In the Bi 2:2:1:2 system, T_c depends strongly on the oxygen content x: It has a maximum of about 95 K for an oxygen content of $x \approx 8.16$.[24] By appropriate annealing it is possible to vary T_c between ≈ 75 and 95 K for MCP samples and between 55 and 95 K for Pb-doped sintered samples.[16,17] It is far easier to decrease T_c by increasing the oxygen content of sintered samples than of MCP samples, because the oxygen mobility is much larger in the porous sintered material than in the dense MCP samples.

The morphology of samples KnBock1 and KnBock6 is shown in Figs. 1(a) and 1(b), respectively. A comparison with typical sintered material [Fig. 1(c)] shows that the grains are significantly larger and more densely packed in the melt-processed samples. As a result, the intergranular contacts are better and therefore the critical current is larger in melt-processed samples than in sintered samples.[18,19] A comparison between the samples KnBock1 and KnBock6 shows that the additional heat treatment did not change the morphology.

Samples Bo105a and Bo105b are also obtained by the MCP. After melt casting they were annealed for 24 h in an N_2/air mixture (1:1) at 750 °C and then for 130 h in air at 850 °C. The powder sample Bo5/8 is also a MCP sample.

The sample KaMu96 was prepared by a similar technique:[17] The appropriate mixture of metal oxides was prereacted in an aluminum oxide crucible for 60 h at 780 °C. The product was melted for 2 h at 1050 °C and poured into a quartz mold. It was then annealed for 23.5 h at 770 °C and for 288 h at 850 °C in air and afterwards cooled down slowly to room temperature (1 °C/min).

The sample 162Ox was prepared at the Institut für Anorganische Chemie, Universität zu Köln, by a different technique: The appropriate mixture of pure metals [Bi,Cu ($\geq 99.99\%$) and Ca,Sr ($\geq 99\%$)] was at first arc melted; then the regulus was ground and subsequently annealed in an O_2/Ar gas stream.[20,21]

The oxygen content of the series of MCP samples KnBock1–KnBock6 and Bo105a and Bo105b was determined by iodometric titration analysis by Hüdepohl and Bock.[23,19] The results and the respective T_c's are shown in Table I. The correlation between x and T_c is consistent with the results published in Ref. 24.

All samples have been characterized by x-ray, resistivity, and ac-susceptibility measurements. In general, all samples are single phase by the quality criteria given in Ref. 16. However, for sample KaMu96 the peaks in the diffraction pattern are quite broad and samples KnBock1–KnBock6 have a small contribution of the Bi 2:2:2:3 phase, which shows up in high-field susceptibility data, but can hardly be detected by the other characterizations.

Normal-state susceptibility and magnetization curves of samples Ne41T10B, KnBock(1–6), Bo105a, and KaMu96 were measured in fields up to 1.35 T with a Faraday balance. The susceptibility above T_c consists of a temperature-independent term of about 2×10^{-7} cm^3/g and a weak Curie-Weiss contribution, which is observed in most of the samples. Regarding the series KnBock(1–6), the Curie-Weiss contribution vanishes in those pieces which are annealed in Ar (i.e., which have the highest T_c and the lowest oxygen content). Such a dependence of the normal-state susceptibility on the oxygen content is known and is caused by intrinsic Cu^{2+} moments and not by foreign magnetic impurities.[24] Therefore the susceptibility data of our samples give no evi-

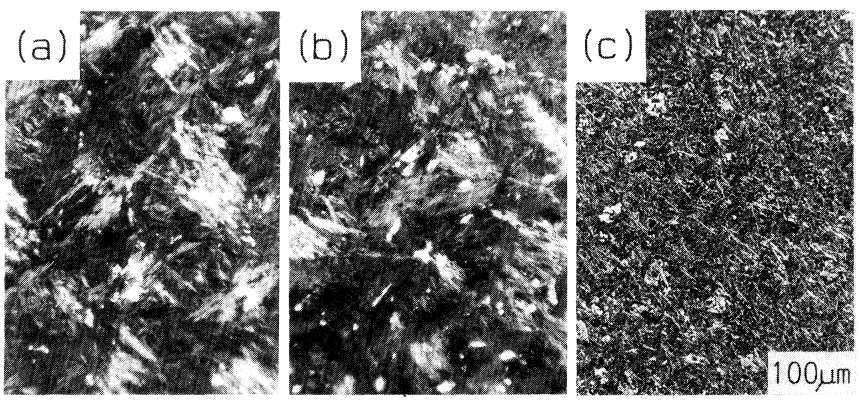

FIG. 1. Morphology of melt-processed and sintered Bi 2:2:1:2 samples: (a), (b) melt-processed samples KnBock1 and KnBock6, respectively. Sample KnBock6 is a piece of sample KnBock1, which was additionally annealed in Ar. The morphology was not changed by this additional heat treatment. (c) A typical sintered sample.

TABLE I. Oxygen content x and T_c of $Bi_2Sr_2CaCu_2O_x$ samples. The correlation between x and T_c is consistent with the results published in Ref. 24.

Sample	x	T_c
KnBock1	8.182	84
KnBock2	8.220	81
KnBock3	8.189	83.5
KnBock4	8.186	87
KnBock5	8.178	91
KnBock6	8.169	93
Bo105a	8.161	94.5
Bo105b	8.126	89

dence for foreign isolated magnetic impurities.

The magnetization curves for $T > T_c$ are linear and extrapolate to zero for $H \rightarrow 0$. The experimental uncertainty for the intercept M_0 of the extrapolation is about 2×10^{-4} G (which corresponds, e.g., to the saturation moment of ≈ 0.14 ppm iron at room temperature).

In order to investigate the microstructure of the samples, the contents of the cations of samples Ne41T10B, KnBock1, KnBock6, Bo105a, Bo105b, and KaMu96 were studied by high-resolution energy-dispersive x-ray (EDX) analysis in a transmission electron microscope.[25] All samples were powdered in a mortar and were measured on a carbon-film-covered molybdenum grid. From each sample the cation content (Bi,Sr,Ca,Cu) of 50 small crystals (electron diffraction) with sizes of 2000–7000 Å was measured. From these data the mean and standard deviations of the stoichiometric distribution with respect to the cations (Bi,Sr,Ca,Cu) were calculated for each sample.

In general, the well-known nonstoichiometry of Bi 2:2:1:2 was observed: The content of Bi, Sr, Ca, and Cu was found to scatter around 10–15 %.

The standard deviation of the stoichiometric distribution of all cations is higher (about twice) in most of the MCP samples than in sintered samples. However, in the case of the MCP sample KnBock6, which was additionally annealed in Ar for a long time (and actually exhibits a paramagnetic Meissner effect; see below), the standard deviation is nearly equal to the one of the sintered samples (such as, e.g., Ne41T10B).

The analysis of all 300 measured crystals shows an exchange of Ca and Sr ions in the stoichiometric distribution which roughly obeys the rule $BiSr_{2+x}Ca_{1-x}CuO_{8-\delta}$.[25] However, it reveals no significant difference either between sintered samples and MCP samples in general or between samples with and without the PME.

III. EXPERIMENTAL DETAILS

Our measurements of the low-field dc susceptibility were performed with a special SQUID magnetometer. Since conventional SQUID susceptometers have sometimes been reported to produce artificial paramagnetic moments in the superconducting state,[26] we have made an extensive effort to exclude such experimental errors. We shall therefore describe our apparatus in some detail.

We use a commercial *rock magnetometer,* which works with a rf SQUID but without a superconducting magnet.

The magnetometer is positioned inside a double wall of Mu metal, which shields the Earth's field to $\approx 99\%$. The residual field at the sample position was measured by axial and transversal Förster probes.[27,28] Both $H_{\parallel}$ and $H_{\perp}$ were found to be lower than 1 mOe. To have an absolute value of the magnetic moment, the output signal was calibrated by a short copper coil.

In its conventional mode, rocks at room temperature are moved mechanically through the sample-access hole into the SQUID-sensitive region. The SQUID pickup coils are wound Helmholtz-like to achieve a ≈ 3-cm-wide region in which the signal is not sensitive to the sample position.[29] The pickup coils and the SQUID device are surrounded by a superconducting shield. The measurements are usually performed in zero external field.

For our investigations we have added a cryogenic insert for measurements at low temperatures and Helmholtz coils to apply a low external dc field. The latter surround the whole magnetometer and are sited within the Mu-metal shield, but outside the superconducting shield. The cryogenic insert is made of nonmagnetic and *nonmetallic* materials (mainly glass). Metallic materials are not recommended because differential thermocurrents can produce noise in the SQUID signal. The only metal in the sensitive region is the metallic part of the thermometer (a Si diode, which is fixed next to the sample) and its leads.

The dc field is applied when the superconducting shield is heated to its normal state. It is then trapped in the shield when this is cooled down again.

The cryogenic insert holds the sample mechanically fixed at the center of the pickup coil system. The sample is cooled by a He-gas stream. The SQUID signal is then recorded while changing the temperature. Note that the sample is *never moved* during the measurement. This guarantees that the sample *does not experience any change* of the external field. This is an essential point, since sample movement in an *inhomogeneous* field (e.g., residual fields of a superconducting magnet in commercial SQUID susceptometers, which is, of course, not present here) can produce apparent paramagnetic moments while the sample is in reality weakly diamagnetic as explained in Ref. 26.

For Bi 2:2:1:2 or Bi 2:2:2:3 samples, the common run proceeds as follows.

(a) Zero-field cooling (ZFC): First, the sample is cooled down in zero field ($|H| < 1$ mOe) to a temperature far below T_c (i.e., 20 K for $T_c \sim 100$ K). Then the field is applied and the sample is warmed up to at least 120 K, i.e., well above the T_c of the Bi 2:2:2:3 phase.

(b) The field-cooled (FC) signal is recorded while the sample is again cooled down in the same field.

A typical result for a Bi 2:2:1:2 sample is shown in Fig. 2. While the screening in the ZFC mode is complete, the dc Meissner flux expulsion (FC mode) is incomplete. No significant field dependence is visible in this very-low-field range (10–100 mOe). Such observations are typically made in HTS's.[2–4,7] Note that the screening in the ZFC

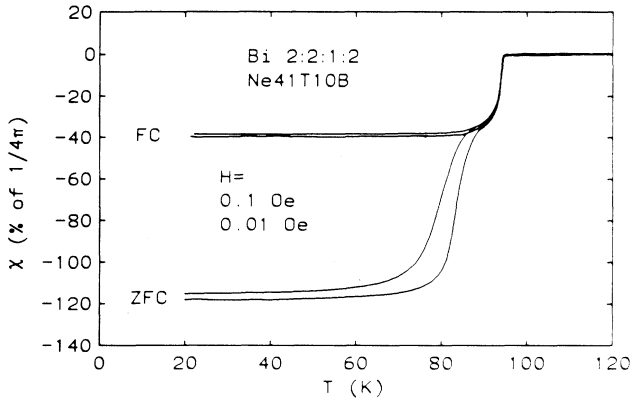

FIG. 2. Zero-field-cooled (ZFC) and field-cooled (FC) susceptibilities as a function of temperature of a high-quality ceramic Bi 2:2:1:2 sample in very low fields. The reduced FC flux expulsion resembles the behavior commonly observed at intermediate fields (about 10–100 Oe).

mode is larger than 100% of $-1/4\pi$. The reason is that the screening currents, which are *induced* by applying the field below T_c at the start of the measurement, screen also voids present in those granular materials. Therefore the screened volume is larger than the effective volume with respect to the mass of the sample as calculated by the x-ray density.

In order to achieve additional information concerning the weak-link structure of our samples, the microwave absorption (MWA) was measured for some of the samples. The measurements were carried out with a conventional Bruker electron-spin-resonance (ESR) spectrometer operated at 9.3 GHz. The microwave power which was applied to the sample was at a level of 10 μW. Additionally, a small dc field and a small low-frequency modulation field (10–100 kHz) with the amplitude varying from 0.1 to 1 Oe were applied. In this way the differential MWA dP/dH can be measured as a function of the applied field and temperature (for details, see Ref. 30).

IV. RESULTS

A. dc susceptibility

In striking contrast to the susceptibility of the sintered sample Ne41T10B (Fig. 2), the one of the melt-processed sample KnBock1 (both Bi 2:2:1:2) shows surprising features (see Fig. 3): While the ZFC susceptibility is comparable to the one of sintered samples, the FC susceptibility exhibits a strong field dependence: The flux expulsion decreases with decreasing field, and in fields lower than 0.5 Oe the susceptibility even becomes *paramagnetic.*

Taking into account the precautions regarding the experimental setup as described in Sec. III, we have to attribute this observation to a real effect of this sample. However, to be absolutely sure, we repeated the experiment with this sample KnBock1 in other laboratories (ETH Hönggerberg in Zürich and Universität Konstanz), which also have SQUID magnetometers in which the magnetic moment can be measured without moving the sample. In these laboratories measurements were performed in fields of 0.1 and 0.17 Oe, respectively, with two opposite field polarities. A paramagnetic magnetization was confirmed in all cases.

Furthermore, we note that the FC magnetization was also measured in our vibrating-sample magnetometer (VSM) (i.e., with a different technique) and the results in the overlapping field range were consistent with the SQUID results, especially including a paramagnetic moment in $H=0.1$ Oe [see Fig. 3(b)].

Therefore we are confident that the appearance of a paramagnetic moment in certain samples is a real effect and not a consequence of experimental drawbacks.

Another point that should also be considered is the possibility that such a result may originate from a nondipole character of the sample. In that context Guy, Strom-Olsen, and Cochrane[31] could show that an antiferromagnet (with vanishing dipole moment) does produce a weak but nevertheless nonzero magnetic flux $\Phi(z_0)$ through the pickup coils of a SQUID magnetometer, which originates in a quadrupole moment. They point out that the contribution of various multipoles to $\Phi(z_0)$ depends on the given arrangement of the pickup coils and on the position z_0 of the sample on the axis of the pickup coil system in the following way: If $h(z_0)$ is the field which would be produced at the sample position z_0 if unit current flowed in the pickup coils, then $\Phi(z_0)$ is proportional to $h(z_0)$ for a dipole, to $h'(z_0)=[dh_z(z)/dz]_{z=z_0}$ for a quadrupole, to $h''(z_0)=[d^2h_z(z)/dz^2]_{z=z_0}$ for an octupole, and so on.[31] In the case of a conventional astatic pair of pickup coils, the sensitivity for a dipole moment is therefore largest in each of the coils and the sensitivity for a quadrupole moment is nonzero at these positions.

In our case, however, the pickup coils are arranged like a pair of Helmholtz coils with a rather large diameter of 50 mm (see Sec. III), so that $h_z(z_0)$ is very uniform at the sample position in the center of the pickup coil system. On the other hand, the sensitivity for nondipole contributions is generally reduced by the large ratio between the pickup coil diameter and the sample size (at least 10). We therefore expect no significant contribution from the leading terms in a multipole expansion of a certain sample except that of the dipole contribution, even if higher harmonics are present.

Furthermore, in case of our sample KnBock1, the PME was confirmed in three other equipments with different pickup coil arrangements (VSM with four pickup coils after Mallinson,[32] SQUID magnetometer in Zürich with an astatic pair of pickup coils, and SQUID magnetometer in Konstanz with planar pickup coils formed like an "∞"[33]). Since the sensitivity for possible higher harmonics of a multipole expansion strongly depends on the special arrangement of the pickup coils, the comparable results of the same sample in different equipments provide evidence that the dipole contribution of this sample dominates the flux measured by most of the common types of pickup coil systems—at least in fields down to 0.1 Oe.

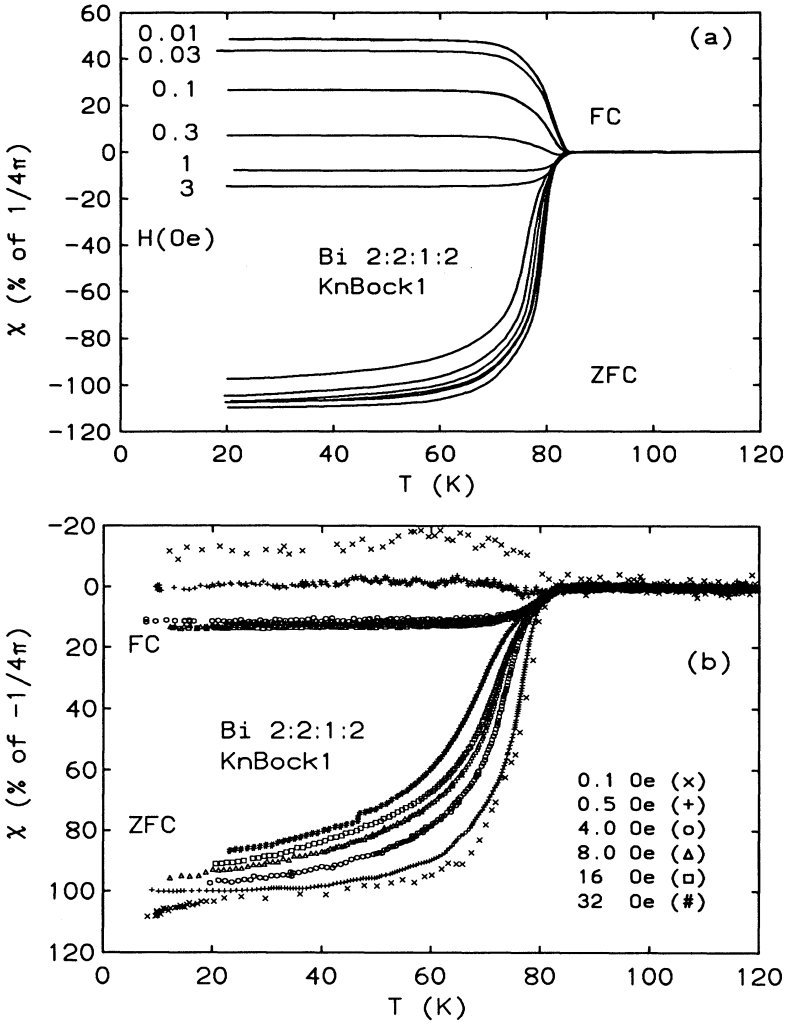

FIG. 3. (a) ZFC and FC susceptibilities as a function of temperature of a melt-processed Bi 2:2:1:2 sample exhibiting the paramagnetic Meissner effect (PME) in very low fields. (b) ZFC and FC susceptibilities of the same sample also taken in higher fields by our vibrating-sample magnetometer.

However, we cannot exclude a certain contribution of higher harmonics in even lower fields ($H \approx 10$ mOe), which could, in principle, show up in equipments other than ours. In fact, we expect a significant antiferromagnetic or glassy nature of the magnetization of PME samples for $H \rightarrow 0$ (see Sec. V).

Note, however, that in case of HTS's special care is needed if one wants to investigate a possible multipole character of a sample, since the movement of the sample can change the magnetization of the sample by induced currents if inhomogeneities of the *applied field* are present.

Obviously, this paramagnetic Meissner effect is not a universal property of Bi 2:2:1:2 generally (e.g., it is not observed in sample Ne41T10B; see Fig. 2). However, it is perfectly reproducible in the special samples such as KnBock1: The measurement for $H = 0.1$ Oe was repeated several times, partly with slightly changed conditions. In one run the field was already applied at room temperature and only the FC susceptibility was measured. Another run was performed with reversed external field

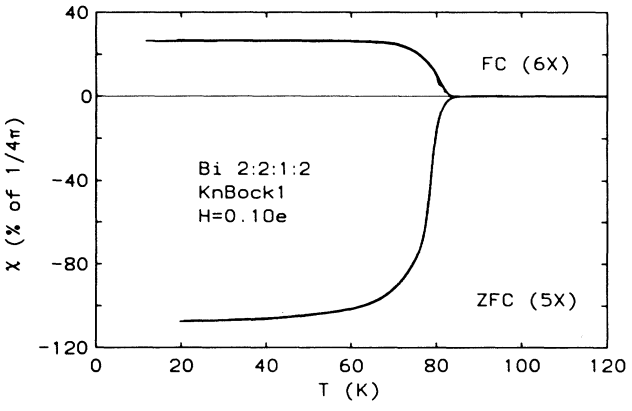

FIG. 4. ZFC and FC susceptibilities as a function of temperature of the PME sample KnBock1 for $H = 0.1$ Oe. Note the perfect reproducibility of the data of the six independent measurements. In some runs the procedure was slightly varied (see text).

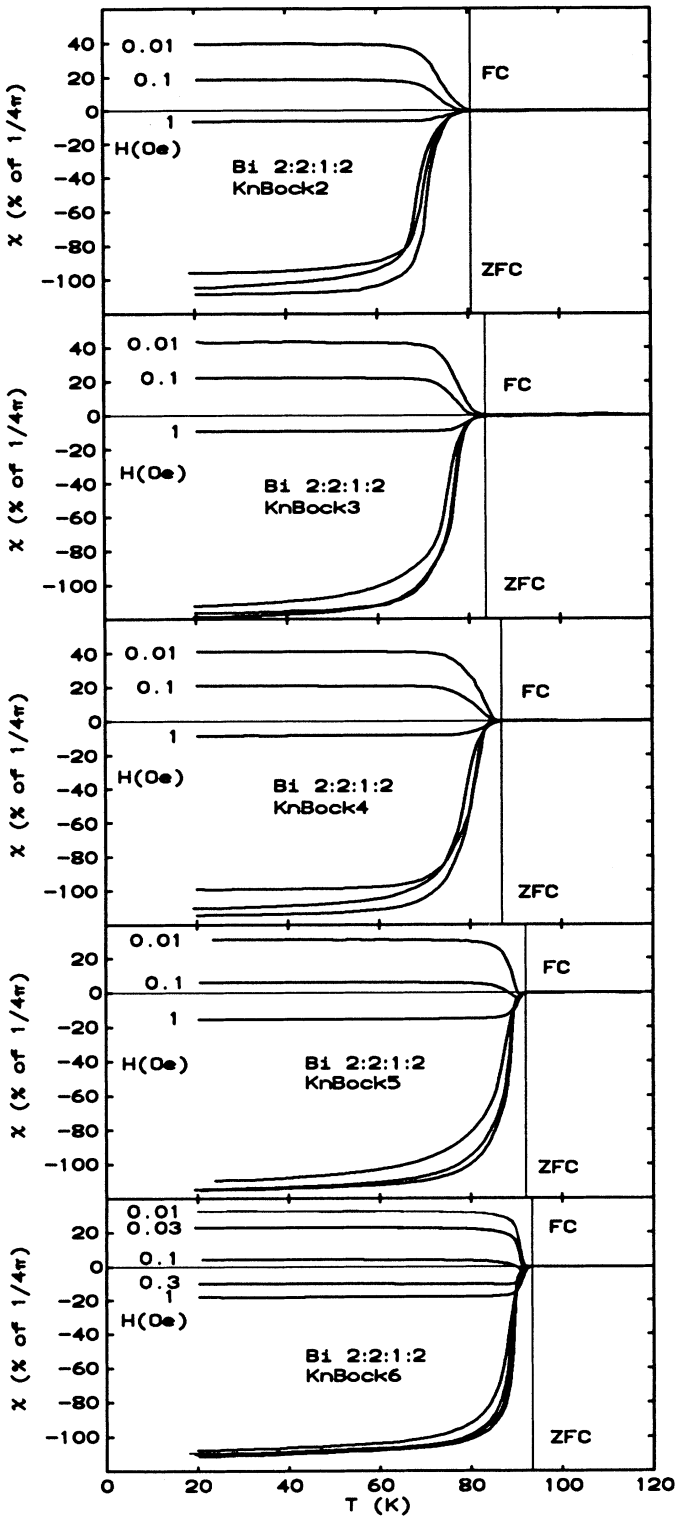

FIG. 5. ZFC and FC susceptibilities as a function of temperature of five melt-processed samples with different T_c's due to appropriate additional annealing of samples of the same batch (KnBock1) in O_2 and/or Ar. The development of the paramagnetic moment in the FC mode is clearly correlated with the particular T_c, which is varied between 80 and 95 K.

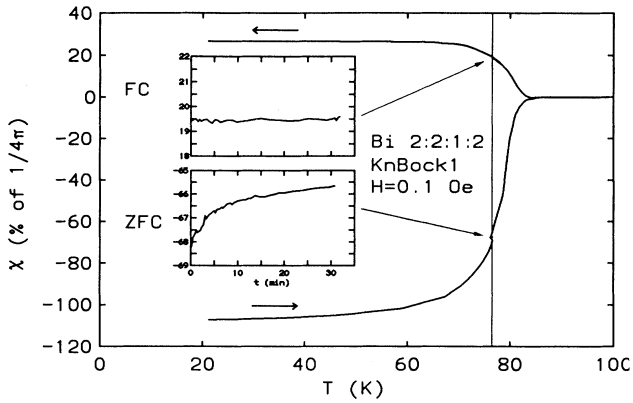

FIG. 6. Measurement of the thermal stability of the PME of sample KnBock1. The temperature was kept at 77 K for $\frac{1}{2}$ h both in the FC as well as in the ZFC branch. The insets show that the ZFC magnetization significantly decreases in time, whereas the FC magnetization does not change in time.

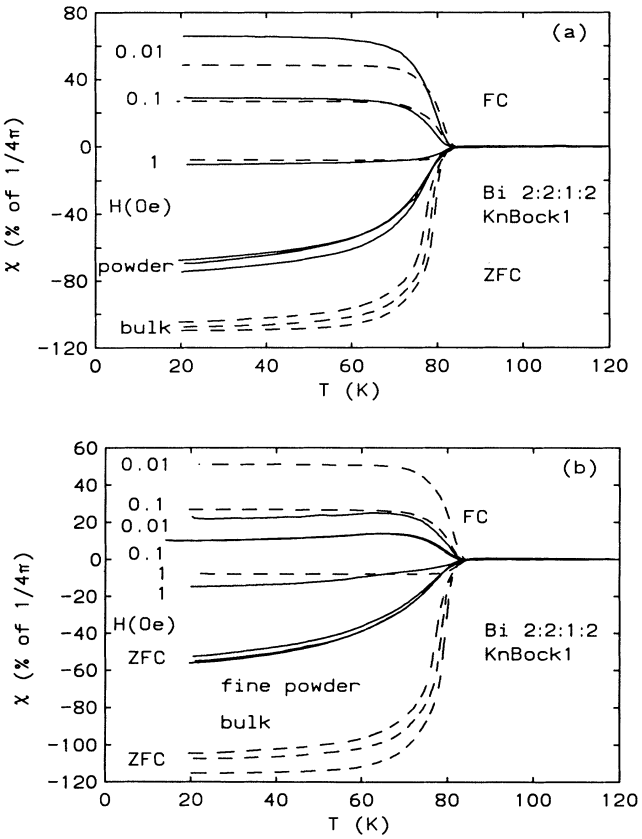

FIG. 7. ZFC and FC susceptibilities as function of temperature of the powered sample KnBock1: (a) Rough powder: The PME of sample KnBock1 is not reduced in powder (solid line) with respect to the bulk (dashed line), but even slightly increased in the lowest field of 10 mOe. The mean diameter of the grains is 2–3 μm. (b) Fine powder: The PME is partially suppressed compared to the bulk (dashed line) and the powder shown in (a).

direction (for which the magnetization changed sign). Finally, the measurement was repeated after the sample had been stored at room temperature outside the magnetometer for 3 weeks. Altogether six runs were performed. The results of all these runs are shown in Fig. 4. They coincide exactly in all cases.

In Fig. 5 we show a set of data of samples KnBock2–KnBock6. These samples originated from sample KnBock1; their T_c's were shifted by additional heat treatments as described in Sec. II. One can see that the low-field susceptibility behavior in general is the same for all the samples. The PME is not destroyed by the heat treatment. Furthermore, one clearly sees that the paramagnetic moment develops right at the respective T_c. This demonstrates that it is correlated with the onset of superconductivity and excludes any explanation of the PME by an independent magnetic effect which might have its critical temperature at T_c just by chance.

To check the thermal stability of the PME, the SQUID signal was observed for 30 min at constant temperature. We chose 77 K, a temperature well below T_c but larger than the temperatures at which the moment is saturated. While the diamagnetic ZFC magnetization decreased clearly for $\approx 3\%$, no significant change of the paramagnetic FC magnetization was observed (Fig. 6). The change of the diamagnetic ZFC magnetization is typical for granular HTS's and can be explained by some flux creep, because the *induced* ZFC magnetization is not the thermodynamic equilibrium. The fact that the paramagnetic FC magnetization does not change with time is evidence that it corresponds to an equilibrium state of the sample.

After these measurements one part of the sample was roughly ground. The grains had a mean diameter of 2–3 μm as investigated by transmission electron microscopy (TEM), but the size of individual grains scattered by a factor of ~ 5. This powder, in which the grains were in loose mechanical contact, shows qualitatively similar results as the bulk material [Fig. 7(a)]. The ZFC signal is reduced, as expected from the destroyed intergranular contacts, while the FC signal in the lowest field of 10 mOe is actually somewhat increased with respect to the bulk signal.

The susceptibilities of a much more thoroughly ground part of the sample are shown in Fig. 7(b): The ZFC signal is further reduced, indicating fewer particles consisting of several grains. The FC data show a significantly *reduced* PME in this powder. The observation that grinding can suppress or even destroy the PME is confirmed by results obtained in Hamburg too. This group worked with powders of well-defined grain sizes.[34] Therefore the PME is obviously an effect of the weak-link network of bulk samples, which is absent in very fine powders.

Besides these rather detailed data of sample KnBock1 (including annealed and ground pieces), which showed the most pronounced PME, for completion we also will present our data of other melt-processed samples.

Samples Bo105a and Bo105b were prepared from the same batch; i.e., their preparation was nearly identical. The only difference is the following: Sample Bo105a was manufactured by annealing a full rod ($\varnothing = 13$ mm, $L = 50$ mm) which was obtained after melt casting. In contrast, sample Bo105b was prepared by annealing thinner slices (1.3 mm thickness) which were cut from the original ingot. The annealing conditions were equal for both samples, yet the access of oxygen during annealing was different for both materials because of the different thicknesses. This affects the growth rate of the two-layer material and may also affect its properties.

In any case, the oxygen content is different for both samples. For sample Bo105a it is $x = 8.161$, close to the value for which T_c reaches its maximum of about 95 K in this system.[24] The oxygen content of sample Bo105b is lower ($x = 8.126$) and its T_c is 89 K (see Table I). The oxygen content probably has a strong influence on the intergranular contacts: The measured critical-current density J_c (which is dominated by the intergranular contacts) of sample Bo105b is lower than that of sample Bo105a by a factor of 200. The difference in the low-field FC susceptibility (Fig. 8) is striking: While sample Bo105a exhibits a pronounced PME, sample Bo105b is diamagnetic in all fields with a saturation value of $\approx 40\%$ of full flux expulsion, which is comparable to the flux expulsion of the non-PME sample Ne41T10B. Only at the lowest field of 10 mOe is the flux expulsion of sample Bo105b slightly reduced, indicating probably an emerging onset of the PME. This result may tell us that intergranular contacts with rather high critical currents are essential for the occurrence of the PME (or that the PME for low J_c is shifted to much lower fields as perhaps indicated by the reduced diamagnetic moment of sample Bo105b in 10 mOe with respect to higher fields).

This deduction, however, seems to be inconsistent with the result of sample KaMu96: While the latter shows a quite pronounced PME with paramagnetic FC magnetization already at 0.3 Oe (similar to KnBock1), it exhibits a strong-field dependence of the ZFC susceptibility (Fig. 9). This probably indicates intergranular contacts with rather *low* critical currents,[16] which can be easily induced by a low field. However, the imaginary part χ'' of the ac

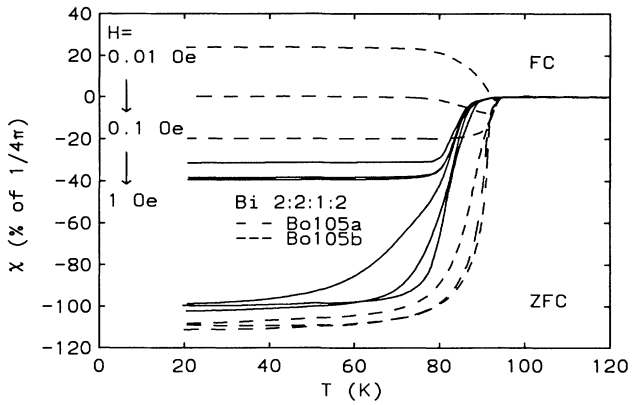

FIG. 8. Low-field susceptibility as function of temperature of two melt-processed Bi 2:2:1:2 samples. Sample Bo105a (dashed line), which shows a pronounced PME, has a ≈ 200 times higher critical transport current than sample Bo105b (solid line), which shows no (or at least a strongly suppressed) PME.

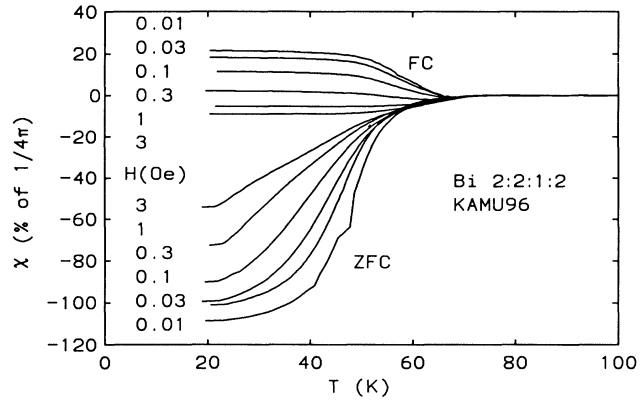

FIG. 9. ZFC and FC susceptibilities as function of temperature of sample KaMu96. This sample shows a quite pronounced PME (already at 0.3 Oe like sample KnBock1). However, the strong-field dependence of the ZFC susceptibility indicates intergranular contacts with low critical currents (see text).

susceptibility exhibits a broad maximum below T_c,[35,33] indicating a broad distribution of critical currents in this sample.

Figures 10(a) and 10(b) show data of a Bi 2:2:1:2 melt-processed powder sample of two different grain sizes, grades 1 and 3, with an average grain size of 1 and 3 μm, respectively. For the finer powder grade 1 [Fig. 10(a)], the FC susceptibility at 20 K is diamagnetic for all fields. However, for the lowest field of 10 mOe, there is a paramagnetic bump near T_c with a width of $\approx$20 K. Such a slight maximum of the paramagnetic low-field FC susceptibility is also seen in the data of the powder grade 3 [Fig. 10(b)] and in those of the fine powder of KnBock1 [see Fig. 7(b)] (although in these cases the susceptibility remains paramagnetic at lower temperatures). Note that the strong suppression of the PME in the fine powder grade 1 in comparison with grade 3 confirms the general tendency stated above. Besides this, we tend to attribute the decrease of the paramagnetic moment with decreasing temperature visible in these figures to the usual development of the background diamagnetism: For the case that the size of the particles in the powder is comparable to the London penetration depth λ, the diamagnetic moment develops smoothly as λ decreases with decreasing temperature. This temperature dependence of the diamagnetic moment can be observed both in the ZFC and FC susceptibilities (with $H=1$ Oe) in Figs. 10(a) and 10(b). If the paramagnetic moments, which are believed to be embedded in a diamagnetic matrix (see Sec. V), saturate at low temperatures as in the bulk samples, the remaining temperature dependence is due to the diamagnetic matrix.

Another Bi 2:2:1:2 sample under study was prepared by melting a mixture of pure metals (instead of metal oxides) and subsequent heat treatment (see Sec. II). Although its FC susceptibility remains diamagnetic even in the lowest field, there is a strong tendency toward a paramagnetic magnetization with decreasing fields (Fig. 11). Since we have shown a lot of undoubtedly paramag-

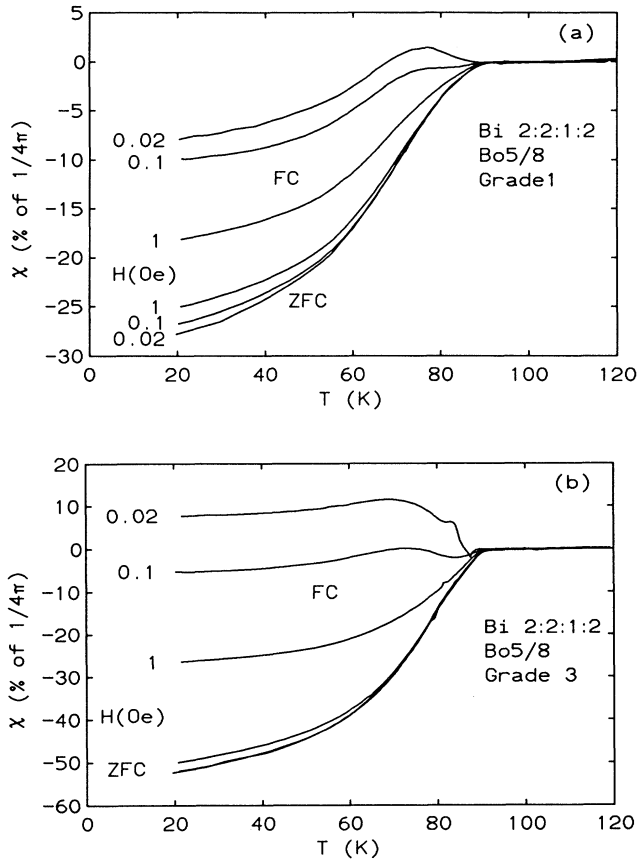

FIG. 10. ZFC and FC susceptibilities as function of temperature of the melt-processed powdered sample Bo5/8 with two different grain sizes: The mean grain size of (a) sample Bo5/8 grade 1 is 1 μm and that of (b) sample Bo5/8 grade 3 is 3 μm. The PME is strongly suppressed in very fine powders (compare with Fig. 7), and the paramagnetic magnetization decreases with decreasing temperature (see text).

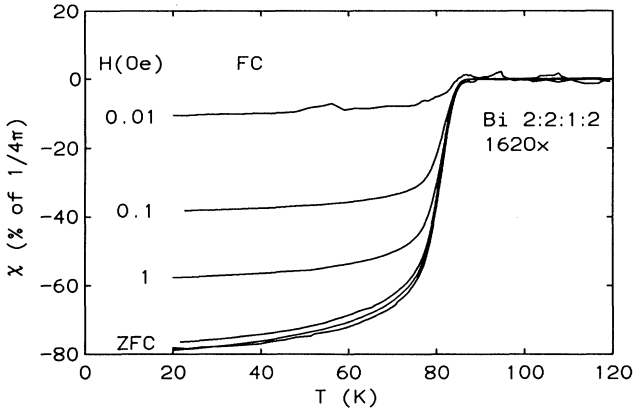

FIG. 11. Low-field susceptibilities as function of temperature of a Bi 2:2:1:2 sample prepared by melting a mixture of pure metals before the final heat treatment. Although the magnetization is diamagnetic in all fields, the tendency points toward a PME behavior.

netic FC magnetizations, it seems reasonable to attribute this behavior to the onset of the PME rather than to reduced flux expulsion due to field-dependent flux trapping or pinning. A real paramagnetic magnetization would probably develop at an even lower field which is not accessible in our equipment. In this context it should be noted that, in principle, the PME may account for each observation of a reduced (while still diamagnetic) Meissner effect in HTS's in very low fields.

An interesting feature of all samples which show the PME is the temperature dependence of the FC branch close to T_c: The FC moment first follows the ZFC branch to diamagnetic values, and only at a certain temperature T_d of order 1 K below T_c it does deviate and turns up to paramagnetic values. This dip is observed in all samples which show the PME. In Fig. 12, as an example, we show results of sample KnBock6. T_d is obviously field dependent, and the dip is deeper in higher fields. In this sample one can see a similar feature even in the ZFC branch. It develops a steplike temperature dependence, and in the lowest field it has even a local maximum just below T_c.

Up to now we discussed the behavior of different samples of the Bi 2:2:1:2 compound. However, the PME is not uniquely restricted to this system. In Fig. 13 we present the data of sample Kn75KA. It is a ground sample (grain size ≈ 4 μm) *of the Bi 2:2:2:3 structure with* $T_c \approx 110$ K. The FC susceptibility below T_c becomes paramagnetic in fields $H < 0.05$ Oe; an onset of the PME is, however, visible already at 0.1 Oe. The discovery of the PME in this sample was actually guided by an anomaly in the low-field microwave absorption, which is apparently correlated with the PME (see below). We also remind the reader here again of several reports (mentioned in the Introduction) about the PME in different systems.

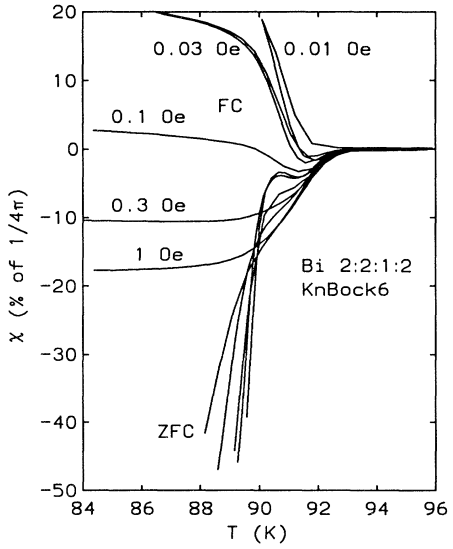

FIG. 12. Temperature dependence of the FC susceptibility of a PME sample close to T_c. Results of sample KnBock6 are shown as an example; however, the diamagnetic dip just below T_c is observed in all PME samples.

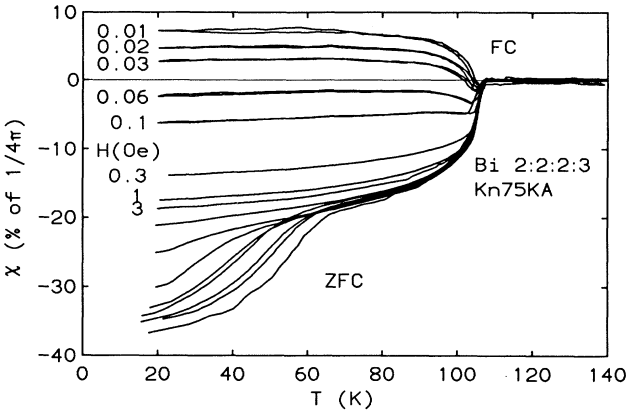

FIG. 13. ZFC and FC susceptibilities as function of temperature of the Bi 2:2:2:3 sample Kn75KA, which also shows the PME. The PME is not a unique property of only Bi 2:2:1:2 samples.

In order to investigate the field dependence of the FC susceptibility of samples with the PME, we have collected the values of sample KnBock1 at low temperatures (20 K). The data are shown in Fig. 14. The x axis of the plot is logarithmic, because the applied field varies between 10 mOe and 10 kOe (six orders of magnitude). The points indicated by (○), (∗), and (△) represent FC measurements performed in the SQUID magnetometer [most of them shown in Fig. 3(a)], in the vibrating-sample magnetometer [Fig. 3(b)], and in a Faraday balance, respectively. For comparison, we also show the respective data for the sintered sample Ne41T10B, which does not show the

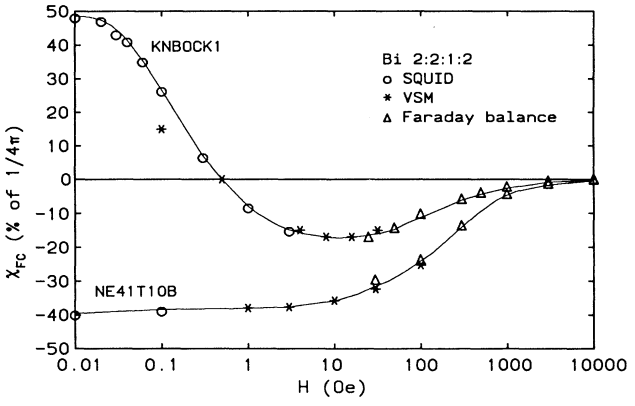

FIG. 14. Field dependence of the FC susceptibility of the melt-processed sample KnBock1 and of the sintered sample Ne41T10B at 20 K. The applied field was varied between 10 mOe and 10 kOe (six orders of magnitude). The measurements were performed with the SQUID magnetometer, the vibrating-sample magnetometer, and a Faraday balance. The field dependence is qualitatively equivalent in fields $H > 10$ Oe for both samples, but whereas the FC susceptibility of sample Ne41T10B remains constant in fields $H < 10$ Oe, the PME of sample KnBock1 emerges in fields $H < 2$ Oe. The solid lines are guides to the eye.

PME. The solid lines are guides to the eye.

Besides the low-field range, the field dependence is qualitatively equivalent for both samples: Starting at our highest field of 10 kOe ($\gg H_{c1}$), the flux expulsion increases with decreasing field and saturates in fields of order 10 Oe ($<H_{c1}$) at $\approx 40\%$ of $-1/4\pi$ for sample Ne41T10B and at $\approx 17\%$ of $-1/4\pi$ for sample KnBock1. Whereas the FC susceptibility of sample Ne41T10B remains constant in lower fields, in the case of sample KnBock1 it deviates from the plateau of $\approx 17\%$ of $-1/4\pi$ at ≈ 2 Oe, crosses zero at ≈ 0.5 Oe, and increases rapidly with further decreasing field. This behavior is also shown in the linear plot in Fig. 15 for fields $H < 16$ Oe. A reasonable analytical description for this low-field behavior, as suggested by the plot presented in the inset of Fig. 15, is

$$\chi - \chi_0 = \frac{M_s}{(H + H_0)^{\alpha}} , \tag{1}$$

with $\chi_0 = 17\%$ of $-1/4\pi$, $H_0 = 0.16$ Oe, $M_s = 0.095$ G/4π, and $\alpha = 1.05$ close to 1. The solid line in Fig. 15 and the straight line in the inset correspond to this fit.

The same fit applied to the data of the Bi 2:2:2:3 sample Kn75KA yields a somewhat different result, namely, $\alpha = 1.5$, $\chi_0 = 19\%$ of $-1/4\pi$, $H_0 = 0.14$ Oe, and $M_s = 0.015$ G/4π. For sample KaMu96 the fit parameters are $\chi_0 = -11\%$, $H_0 = 0.18$ Oe, $M_s = 0.065$ G/4π, and $\alpha = 0.96$, which is again close to 1.

B. Microwave absorption

Several samples which show the PME also exhibit an anomaly in their low-field microwave power absorption (Fig. 16). In fields below H_{c1}, the microwave absorption (MWA) of HTS's is due to dissipative flux motion in the weak-link network or, equivalently, due to the junction's resistance. The typical field dependence of the measured

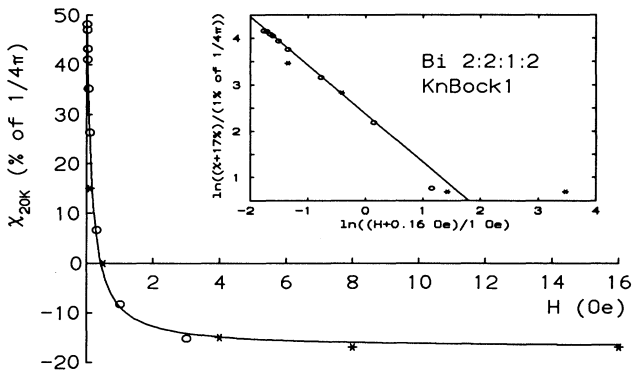

FIG. 15. Field dependence of the FC susceptibility of sample KnBock1 at 20 K. The points indicated by (○) and (*) were taken in the SQUID magnetometer and in the vibrating-sample magnetometer, respectively. The data in the log-log plot in the inset can be fitted by Eq. (1) (with $\alpha \approx 1$), indicating the existence of spontaneous orbital moments, which are field and temperature independent at $T \ll T_c$ and $H < 3$ Oe. This fit also gives the solid line in the linear plot.

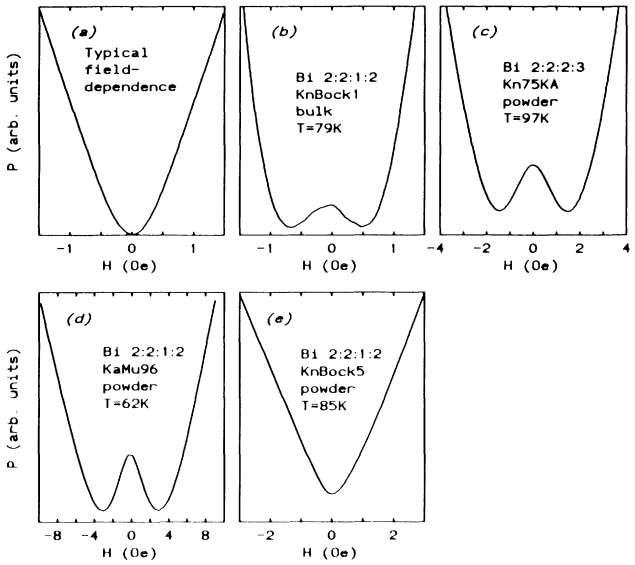

FIG. 16. Magnetic-field dependence of the microwave absorption (MWA): (a) For a typical HTS sample, which does not show a PME. The changeover from parabolic to linear field dependence occurs at the Josephson critical field H_{c1}^* (Ref. 30). (b) For the Bi 2:2:1:2 sample KnBock1, which shows the PME (see Fig. 3). The absorption has a maximum at $H = 0$ and two minima at about ± 0.6 Oe. (c) For the Bi 2:2:2:3 sample Kn75KA, which shows the PME. (d) For the Bi 2:2:1:2 sample KaMu96, which shows the PME. (e) For the Bi 2:2:1:2 sample KnBock5, which shows the PME (for the explanation of this exception, see text).

differential MWA dP/dH in this case is the following: dP/dH increases almost linearly in fields up to a certain field H_{c1}^* of order 1 Oe and is more or less constant, or sometimes decreases, at higher fields. H_{c1}^* is associated with the critical field, at which the magnetic flux breaks into the weak-link network. Then the field penetrates up to the London penetration depth into the grains which were screened before by weak links.[30] Figure 16(a) shows the observed field dependence of the (MWA) $P(H)$ for a sample without the PME, which is obtained from the original $dP/dH(H)$ curve by numerical integration: There is a minimum of the absorption at zero field, followed by a parabolic increase, which turns into a linear increase at fields larger than H_{c1}^* (here about 0.6 Oe). In contrast to this the PME sample, KnBock1 (compare Fig. 3) shows a maximum of absorption at zero field, followed by minima near ± 0.6 Oe [Fig. 16(b)]. This feature appears ≈ 1 K below T_c and disappears ≈ 6 K below T_c. Outside this temperature interval, the MWA resembles that shown in Fig. 16(a). A similar behavior of the MWA was observed in the Bi 2:2:2:3 sample Kn75KA [Fig. 16(c)], and indeed we could detect the PME in this sample in a subsequent measurement with the SQUID magnetometer (see above and Fig. 13).

A pronounced anomaly in the MWA was also found for sample KaMu96 [see Fig. 16(d)].

The anomaly in the MWA is obviously correlated to

the PME. However, it is not seen in the PME samples KnBock2–KnBock6 [as an example, see Fig. 16(e)]. The anomaly is covered by a strong normal MWA. Note that the MWA measurements were performed with increasing dc field, which generated screening currents. It is obvious that the anomaly, which is attributed to the PME, can only be observed at temperatures close to below T_c where the screening is weak.

V. DISCUSSION

Obviously, the PME is a low-field effect and depends on some peculiarities of the given samples. The crucial question is how samples with and without the PME differ from each other.

Some PME samples show an anomaly in the low-field MWA as shown in Sec. IV B. An anomaly of our PME samples recently found in the second harmonic of the ac susceptibility provides another interesting way to detect the paramagnetic magnetization. The results are published in detail elsewhere.[33]

Besides these anomalies, up to now all attempts have failed to find any significant difference between samples with and without the PME in resistivity, specific heat, stoichiometry, structure, and microstructure (see Secs. II and IV). The only fact we have is that all of our PME samples were (at least partially) melted during the preparation. It seems that structural and/or chemical causes, which are responsible for the PME, are very subtle and difficult to detect experimentally.

One can, of course, think about magnetic impurities. However, the PME itself cannot be ascribed to an effect of isolated magnetic impurities. Commonly, the susceptibility due to isolated impurities should be field independent (up to a saturation field which is typically much larger than the fields we are dealing with). Furthermore, the temperature dependence of the susceptibility should be Curie-like: $\chi_{\text{imp}} \sim C/T$. This behavior is definitely not seen in our observations: The measured susceptibility is *temperature independent* (below $\sim 0.8 T_c$) and depends strongly on the applied field [see Eq. (1) and Fig. 15].

One may suspect that we are dealing with small ferromagnetic clusters instead of isolated impurities. For sample KnBock1 the paramagnetic magnetization below T_c with $H = 0.1$ Oe is 2.4 mG. The saturation magnetization of only 1.7 ppm iron (at room temperature) would give the same result. There is, of course, the problem that one has to invoke a flux redistribution at T_c which must produce an unreasonable field enhancement at the position of such ferromagnetic clusters if one wants to explain the PME in this way. However, such ferromagnetic clusters should be detectable in high-field magnetization curves above T_c by an intercept in the extrapolation for $H \rightarrow 0$. But no such intercepts were found for samples KnBock1, Bo105a, and KaMu96 (see Sec. II) within the experimental error of 2×10^{-4} G, which is still 12 times less than the magnetization of sample KnBock1 at $H = 0.1$ Oe and 4 times less than the magnetization of sample KaMu96 at 0.1 Oe. Therefore we can exclude this explanation too.

It is also improbable that the PME originates in a vortex-antivortex separation in combination with a Kosterlitz-Thouless transition,[8] since the paramagnetic susceptibility should develop only very close to below T_c.

Another approach for understanding the PME is based on the assumption of metastable orbital magnetic moments of the grains in the superconducting state: The magnetic behavior of small samples (in our case grains) of superconductors may be rather complicated. For example, the existence of a "giant vortex state" was discussed in Ref. 36. It was even claimed—and observed[36]—that the total magnetic moment of such small samples (in this case disk shaped) may become paramagnetic in FC experiments above T_c but below the temperature T_3, at which the applied field is equal to the upper-surface critical field H_{c3}.

We do not think, however, that this explanation can be applied in our case: The effect discussed in Ref. 36 is due to the formation of a metastable state which implies surface currents, corresponding to the conservation of an adequate orbital quantum number. The results were obtained for type-I superconductors with small κ, whereas we are dealing with extreme type-II superconductors ($\kappa \sim 100$). Furthermore, the theory[36] predicts that the paramagnetic moment should disappear with decreasing temperature when the critical field $H_c(T)$ becomes larger than the applied field. At this temperature the sample should rapidly enter the full Meissner state. This really happened in the experiments shown in Ref. 36. In our case, however, the paramagnetic moment persists down to the lowest temperature ($\ll T_c$). The dependence of the effect on the applied field predicted in Ref. 36 also does not agree with our results [Eq. (1)]. Especially, the paramagnetic moment should disappear below a certain threshold field, whereas our observations (Fig. 2) indicate that it persists down to the lowest fields.

Our suggestion to explain the PME is the idea of the formation of spontaneous magnetic moments (spontaneous currents) in certain samples in the superconducting state. If we discard the possibility that the paramagnetic moment is due to a metastable state as described in Ref. 36, we must assume that the currents and therewith the magnetic moments we observe are really spontaneous: They appear below T_c and persist down to zero temperature as a stable state. In this context we can explain the observed temperature and field dependences. This would also be consistent with the result mentioned above that the PME state seems to be an equilibrium state (Fig. 6).

The data shown in Sec. IV, especially the observation that the PME is suppressed in fine powder, and the MWA anomaly seen in several PME samples give rise to the assumption that these spontaneous currents run through weak links. The anomaly in the MWA can be explained in the following way: If in the absence of any external field there already exist spontaneous currents in the network of Josephson weak links, then the application of the microwave field will induce additional microwave currents. If the sum of the spontaneous current and the microwave current at a certain weak link is larger than its critical current, the additional current can flow only as a result of Giaever tunneling and thus with dissipation. As the field increases, the spontaneous currents vanish together with the paramagnetic magneti-

zation and the absorption decreases. At the same time, the ordinary MWA caused by dissipation in weak links without spontaneous currents increases with increasing field as explained in Sec. IV B. Whether the sum of these two kinds of MWA leads to the "W"-like field dependence shown in Fig. 16, and where its minima are, depends probably on the intensity of the different kinds of MWA and on the number of the respective weak links. The weak links need not necessarily be intergranular contacts. Also, defect planes in single grains or single crystals may have the same effects.

If a field-independent magnetization M_s indeed appears below T_c, the sum of this magnetization and the diamagnetic contribution $(-a/4\pi)H$ would result in a susceptibility

$$\chi = M/H = M_s/H + \chi_0 ,$$

with $\chi_0 = -a/4\pi$. a is the Meissner fraction at higher fields.

If, however, in zero field these spontaneous moments are distributed randomly or ordered by some mutual interaction, leading to a state like that of a spin glass (orbital glass), the average moment will be zero. In fields lower than a certain field H_0, the moment will be more or less linear with the applied field and will saturate in higher fields. The susceptibility M/H will therefore tend toward a finite value for $H \rightarrow 0$ and obey the $1/H$ dependence in fields higher than H_0. Such a curve can crudely be approximated by Eq. (1) (with $\alpha = 1$) as suggested by the fit in Fig. 15.

A possible explanation for the appearance of spontaneous moments could be the existence of weak links with inverse Josephson coupling. There are several theoretical predictions which explain this effect.

It was shown in Refs. 37–39 that if the cooper pair tunneling in a Josephson contact does not proceed directly, but via magnetic impurities in the barrier, the sign of the Josephson coupling

$$E = -J_c \cos(\Phi_1 - \Phi_2)$$

changes; i.e., the critical Josephson current becomes negative ($J_c < 0$). In this case in the ground state the phase difference of the two sides of the contact would not be zero, as usual, but π.

If one now regards a ring (SQUID) with such a π contact, there should be a current and a magnetic moment in the ground state at zero field corresponding to a magnetic flux of $\Phi_0/2$ through the ring. In other words, the dependence of the energy of the current running through the loop with a π contact will be shifted by π in comparison with the ordinary situation.

Detailed calculations given in Ref. 37 show that the phase difference across the weak link in such a ring depends on the inductivity L of the ring and on J_c. A spontaneous flux exists if

$$\frac{2\pi L |J_c|}{c\Phi_0} > 1 . \tag{2}$$

The phase difference π and the corresponding flux $\Phi_0/2$ is obtained in the limit $(2\pi/c)L|J_c| \gg \Phi_0$. Some properties of these contacts were also discussed in Refs. 40 and 41.

Negative Josephson coupling may also appear in disordered superconductors[39] or in a S-N-S junction as a result of a Coulomb interaction if the electron-electron coupling in the normal metal N is repulsive.[42] The additional supercurrent due to the Coulomb interaction[42] dominates the usual one if the normal metal is, e.g., in the ferromagnetic state.

Another possible reason for the appearance of spontaneous currents is the assumption of d-wave pairing in HTS's. Though the pairing of HTS's is usually believed to have an ordinary form (s wave, singlet), several recent results (see, e.g., Ref. 43) have been interpreted as a possible indication of nontrivial pairing in HTS's. If this is true, π contacts may arise in a network of weak links as pointed out by Sigrist and Rice.[44,45] It would be an intriguing result if the PME would turn out to be an indication of nontrivial pairing in HTS's.

Since a granular HTS can be thought of as a network of weak links, the assumption of a certain amount of π contacts among them can qualitatively explain the observed field dependence of the PME as well as the fact that it is not observed in all samples.

The theoretical discussion given in Refs. 37, 44, and 45 shows also that for π contacts the magnetic response just below T_c should be diamagnetic; only when the critical-current density $|J_c|$ reaches a certain critical value [see Eq. (2)] would spontaneous currents appear. Thus there should be a crossover from diamagnetic to paramagnetic behavior at a certain temperature $T_d < T_c$. Exactly such a crossover occurred in our measurements as shown above.

At the moment the microscopic mechanism of the PME is still not clear. However, the models which turned out to be most successful up to now—tunneling via magnetic impurities for ordinary s-wave superconductors[37] or phase mismatch in context with d-wave superconductors[44,45]—both have phenomenologically equivalent consequences: Spontaneous currents and therewith spontaneous moments appear in a granular HTS below T_c as a ground-state property. These models are sufficient to explain our main experimental results, especially the field [Eq. (1)] and the temperature dependence of the susceptibility. They are also consistent with the anomaly in the microwave absorption as discussed above (see also Refs. 44 and 45).

VI. CONCLUSIONS

We have observed that certain particular samples of Bi-based HTS's exhibit a paramagnetic moment in the Meissner state in very low fields (< 1 Oe). This "paramagnetic Meissner effect" (PME) is perfectly reproducible and stable. The temperature dependence is similar to that of the usual diamagnetic moment of the ordinary Meissner effect but with the opposite sign, and like the Meissner effect the PME develops just below T_c.

The PME is apparently not a universal property of the HTS's, but it is nevertheless of fundamental interest, since it gives possible evidence for a novel ground state

with nonzero current in the solid state. Though the nature of the PME is still an open question, we mention that the field and temperature dependences of the paramagnetic moment, as well as the behavior of the microwave absorption, are consistent with the assumption of spontaneous moments in the superconducting state. The possible origin of these moments is discussed, and it is tentatively ascribed to the existence of weak links with inverse Josephson coupling (or negative critical current) in our samples.

ACKNOWLEDGMENTS

We thank T. Teruzzi and A. C. Mota as well as Ch. Heinzel and P. Ziemann for confirming the PME of one of our samples with their SQUID magnetometers. We acknowledge A. Maas for experimental support in connection with the EDX analysis and J. Hüdepohl for the iodometric titration of some of our samples. Finally, we thank L. Lundgren, F. V. Kusmartsev V. Moshchalkov, S. Barnes, L. N. Bulaevskii, A. Larkin, T. Geballe, A. Kampf, and A. Freimuth for valuable discussions. The work in Köln was supported by the Ministerium für Wissenschaft und Forschung of the Land Nordrhein-Westfalen, by the Bundesministerium für Forschung und Technologie (Contract No. 13N5494A0) and by the Deutsche Forschungsgemeinschaft through SFB 341. The work at Kazan was partially supported by the Council for High Temperature Superconductivity through Project No. 91151.

*Permanent address: Zavoiskii Physicotechnical Institute, Russian Academy of Sciences, 420029 Kazan, Russian Federation.

†Present address: Material Research Center, Department of Physics, University of Groningen, Nijenborgh 4, 9747 Ag Groningen, The Netherlands. Permanent address: Lebedev Physical Institute, Russian Academy of Sciences, Moscow, Russian Federation.

‡Deceased.

[1]L. Krusin-Elbaum, A. P. Malozemoff, Y. Yeshurun, D. C. Cronemeyer, and F. Holtzberg, Physica C **153-155**, 1469 (1988).

[2]F. Seidler, P. Böhm, H. Geus, W. Braunisch, E. Braun, W. Schnelle, Z. Drzazga, N. Wild, B. Roden, H. Schmidt, D. Wohlleben, I. Felner, and Y. Wolfus, Physica C **157**, 375 (1989).

[3]S. Ruppel, G. Michels, H. Geus, H. Kalenborn, W. Schlabitz, B. Roden, and D. Wohlleben, Physica C **174**, 233 (1991).

[4]D. Wohlleben, G. Michels, and S. Ruppel, Physica C **174**, 242 (1991).

[5]K. Kitazawa, T. Matsushita, O. Nakamura, Y. Tomioka, N. Motohira, T. Tamura, T. Hasegawa, K. Kishio, I. Tanaka, and H. Kojima, in *Superconductivity—ICSC,* edited by S. K. Joshi, C. N. R. Rao, and S. V. Subramanyam (World Scientific, Singapore, 1990), p. 241.

[6]J. G. Perez-Ramirez, K. Baberschke, and W. G. Clark, Solid State Commun. **65**, 845 (1988).

[7]V. V. Alexandrov, V. V. Borisovskii, T. A. Fedotova, L. M. Fisher, N. V. Il'in, O. K. Smirnova, I. F. Voloshin, M. A. Baranov, and V. S. Gorbachev, Physica C **173**, 458 (1991).

[8]P. Svedlindh, K. Niskanen, P. Norling, P. Nordblad, L. Lundgren, B. Lönnberg, and T. Lundström, Physica C **162-164**, 1365 (1989).

[9]W. W. Lee, Y. T. Huang, S. W. Lu, K. Chen, and P. T. Wu, Solid State Commun. **74**, 97 (1990).

[10]M. D. Lan, J. Z. Liu, and R. N. Shelton, Phys. Rev. B **43**, 12 989 (1991).

[11]J. Zhao, V. Suresh Babu, and M. S. Seehra, Physica C **178**, 432 (1991).

[12]S. Thöming, J. Kötzler, M. W. Pieper, and A. Spirgatis, Verhandl. DPG VI **27**, 912 (1992).

[13]B. Schliepe, M. Stindtmann, I. Nikolic, and K. Baberschke, Phys. Rev. B **47**, 8331 (1993).

[14]H. von Löhneysen (private communication).

[15]W. Braunisch, N. Knauf, V. Kataev, S. Neuhausen, A. Grütz, A. Kock, B. Roden, D. Khomskii, and D. Wohlleben, Phys. Rev. Lett. **68**, 1908 (1992).

[16]N. Knauf, J. Harnischmacher, R. Müller, R. Borowski, B. Roden, and D. Wohlleben, Physica C **173**, 414 (1991).

[17]N. Knauf (unpublished).

[18]E. Preisler and J. Bock, *VDI-TZ-Proceedings Supraleitung und Tieftemperaturtechnik* (VDI-Verlag, GmbH, Düsseldorf, 1991), p. 382.

[19]J. Bock and E. Preisler, Solid State Commun. **72**, 453 (1989).

[20]W. Schauerte, Ph.D. thesis, Universität zu Köln, 1992.

[21]W. Schauerte, H. U. Schuster, N. Knauf, and R. Müller, Z. Anorg. Allg. Chem. **616**, 186 (1992).

[22]W. Schnelle, Ph.D. thesis, Universität zu Köln, 1992.

[23]W. Schnelle, N. Knauf, J. Bock, E. Preisler, and J. Hüdepohl, Physica C **209**, 456 (1993).

[24]C. Allgeier and J. S. Schilling, Physica C **168**, 499 (1990).

[25]B. Freitag *et al.* (unpublished).

[26]F. J. Blunt, A. R. Perry, A. M. Campbell, and R. S. Liu, Physica C **175**, 539 (1991).

[27]F. Förster and K. Stambke, Z. Metallkd. **33**, 97 (1941).

[28]F. Förster, Z. Metallkd. **32**, 184 (1940).

[29]W. S. Goree and M. Fuller, Rev. Geophys. Space Phys. **14**, 591 (1976).

[30]V. Kataev, N. Knauf, B. Büchner, and D. Wohlleben, Physica C **184**, 165 (1991).

[31]C. N. Guy, J. O. Strom-Olsen, and R. W. Cochrane, Phys. Rev. Lett. **42**, 257 (1979).

[32]J. Mallinson, J. Appl. Phys. **37**, 2514 (1966).

[33]Ch. Heinzel, Th. Theilig, and P. Ziemann, Phys. Rev. B **48**, 3445 (1993).

[34]M. W. Pieper (private communication).

[35]Ch. Heinzel (private communication).

[36]F. de la Cruz, H. J. Fink, and J. Luzuriaga, Phys. Rev. B **20**, 1947 (1979).

[37]L. N. Bulaevskii, V. V. Kuzii, and A. A. Sobyanin, Pis'ma Zh. Eksp. Teor. Fiz. **25**, 314 (1977) [JEPT Lett. **25**, 290 (1977)].

[38]L. N. Bulaevskii, V. V. Kuzii, and A. A. Sobyanin, Solid State Commun. **25**, 1053 (1978).

[39]B. Z. Spivak and S. A. Kivelson, Phys. Rev. B **43**, 3740 (1991).

[40]F. V. Kusmartsev (unpublished).

[41]F. V. Kusmartsev, Phys. Rev. Lett. **69**, 2268 (1992).

[42]B. L. Altshuler, D. E. Khmelnitzkii, and B. Z. Spivak, Solid State Commun. **48**, 841 (1983).

[43]J. A. Martindale, S. E. Barrett, C. A. Klug, K. E. O'Hara, S. M. De Soto, C. P. Slichter, T. A. Friedmann, and D. M. Ginsberg, Phys. Rev. Lett. **68**, 702 (1992).

[44]M. Sigrist and T. M. Rice (unpublished).

[45]M. Sigrist and T. M. Rice, J. Phys. Soc. Jpn. **61**, 4283 (1992).

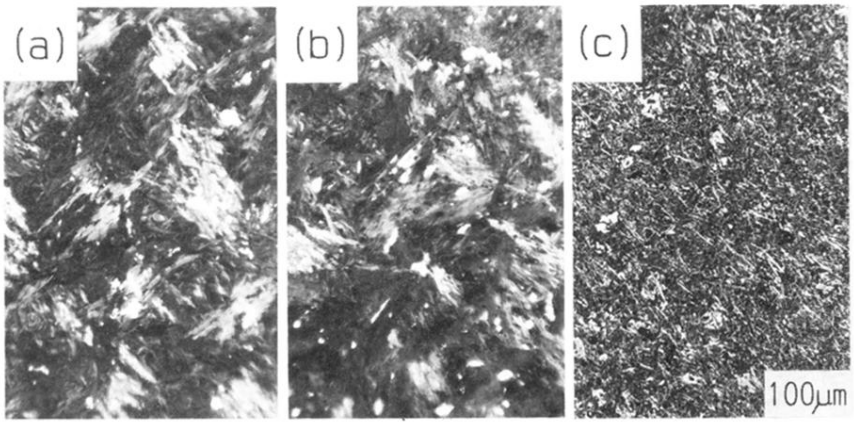

FIG. 1. Morphology of melt-processed and sintered Bi 2:2:1:2 samples: (a), (b) melt-processed samples KnBock1 and KnBock6, respectively. Sample KnBock6 is a piece of sample KnBock1, which was additionally annealed in Ar. The morphology was not changed by this additional heat treatment. (c) A typical sintered sample.